ELSEVIER

Cement & Concrete Composites 24 (2002) 427–435

Cement & Concrete Composites

www.elsevier.com/locate/cemconcomp

# Characterisation of chloride transport and reinforcement corrosion in concrete under cyclic wetting and drying by electrical resistivity

Rob B. Polder *, Willy H.A. Peelen

*TNO Building and Construction Research, P.O.Box 49, 2600 AA Delft, Netherlands*

**Abstract**

Concrete prisms were made with four cement types including cements with fly ash and/or blast furnace slag and three water-to-cement (w/c) ratios. Chloride penetration and corrosion of rebars were stimulated by subjecting prisms to cyclic loading with salt solution and drying. Concrete resistivity, steel potentials and corrosion rates were measured up to one year of age. Chloride penetration profiles were determined after salt loading. It was found that the resistivity of a particular concrete reflects its properties with regard to chloride penetration, corrosion initiation (probability of corrosion) and corrosion propagation (corrosion rate). Blending the cement with blast furnace slag, fly ash or both is beneficial with regard to delaying the onset of corrosion and subsequently limiting its severity under simulated de-icing salt load. The fly ash cement shows increased resistivity compared to Portland cement from eight weeks. Cement with a high percentage of slag develops a significantly higher resistivity after one week.


*Keywords:* Concrete; Reinforcement; Chloride; Resistivity; Corrosion; Blast furnace slag; Fly ash; De-icing salt; Cyclic wetting and drying

## 1. Introduction

Corrosion protection of steel reinforcement in concrete can be lost due to the presence of chloride or carbonation of concrete. For concrete in chloride-laden environments with frequent wetting such as marine submerged and splash zones, the beneficial effects of blended cements are well known [1,2]. Slag and fly ash in the cement delay the onset of corrosion by slowing down the ingress of chloride; after depassivation, they slow down the rate of corrosion. Less well known are the effects of blended cements under less frequent exposure to chloride, such as in de-icing salt environments.

It is well documented that slag and fly ash increase the electrical resistivity of concrete for the same degree of pore saturation. Concrete resistivity is a geometry-independent material property that describes the electrical resistance, that is the ratio between applied voltage and resulting current in a unit cell. Its dimension is resistance multiplied by length (Ωm). Normally low frequency AC ($< 1$ kHz) or DC resistance is considered.

The resistivity of concrete may vary from $10^1$ to $10^5$ Ωm, depending on the moisture content and the concrete composition [3,4]. The current is carried by ions in the pore liquid. Increased pore saturation as well as an increased number of larger diameter pores (higher water-to-cement ratio (w/c)) decrease resistivity. For a constant moisture content, the resistivity increases with time (hydration), and when blast furnace slag, fly ash or silica fume are present. Resistivity also increases when the concrete dries out and when it carbonates, in particular in Portland cement concrete. The effect of an increased chloride content due to salt ingress is relatively small.

From theoretical and experimental work there appears to be a correlation between concrete resistivity and chloride ingress [5,6]. In general, the chloride diffusion coefficient is inversely proportional to the concrete resistivity. Within a particular structure, more permeable zones will have a comparatively lower resistivity and higher chloride penetration.

The resistivity of concrete and the corrosion rate of reinforcement after depassivation are related. Ion transport between anodes and cathodes on the steel surface is one of the rate controlling factors [7]. Simplifying Bazant's model [8], the corrosion rate is inversely proportional to the resistivity [9,10], although this

* Corresponding author. Fax: +31-15-276-3018.
*E-mail address:* r.polder@bouw.tno.nl (R.B. Polder).

0958-9465/02/$ - see front matter 
PII: S0958-9465(01)00074-9

relationship may vary with concrete composition [11–13]. Within a given structure, areas with low resistivity will be associated with a relatively high corrosion rate after depassivation.

## 2. Experimental

Resistivity of concrete made with various cement types including slag and fly ash was studied during and after cycles of exposure to salt solution and drying. Concrete resistivity, steel potentials and corrosion rates were measured. After salt exposure, chloride profiles were taken from the specimens and the remaining parts were exposed to various climates. The cements used are normal Portland cement, fly ash cement, blast furnace slag cement and composite cement with slag and fly ash (further called CEM I, CEM II/B-V, CEM III/B, CEM V/A as by EN 197-1). The concrete compositions are summarised in Table 1. The fine and course aggregate was siliceous river material of 8 mm maximum size. A relatively small maximum size was chosen for optimal grain distribution in the low cover zones (10 mm). This grain size is not typical for bridge decks (usually 32 mm), but it was felt that deviations from behaviour in practice would be limited.

Specimens were prisms of $100 \times 100 \times 300$ mm$^3$ as shown in Fig. 1. Mild steel electrodes for corrosion testing were smooth bars of 8 mm diameter and 150 mm length. They were prepared by light polishing with sandpaper and cleaning in acetone. Then a coat of cement paste and subsequently a coat of dense epoxy coating were given to both ends, leaving an exposed length of 45 mm. Steel bars were positioned at cover depths of 10 or 30 mm. Resistance electrodes were stainless steel (316) screws of 5 mm diameter, positioned at cover depths of 10 and 50 mm. Reference electrodes

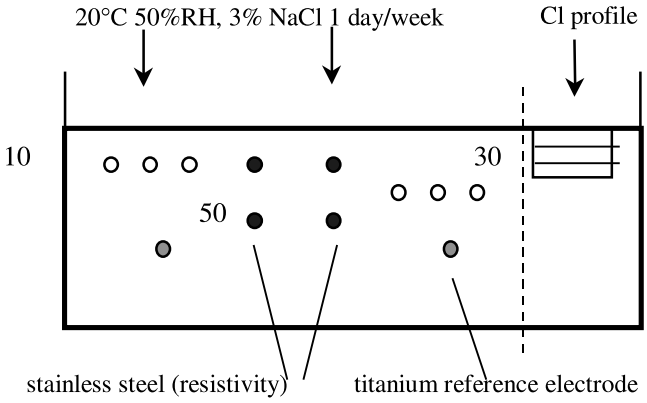


Fig. 1. Prism for de-icing salt exposure with embedded electrodes; concrete was cast from plane above figure; sizes in mm.

were wires of mixed metal oxide coated titanium (Ti*) of 10 mm length with insulated copper wires. The base potential of Ti* electrodes was close to that of Ag/AgCl (saturated KCl). Cubes of 100 mm were used for strength testing.

After demoulding at one day, prisms were stored in a fog room for six days and then exposed in a climate room at 20 °C and 80% RH for three weeks. From four weeks after casting, one face of each specimen was exposed to 26 weekly cycles of 24 h 3% NaCl solution penetration and drying for 6 days in 20 °C and 50% RH. All specimen faces were left unsealed. The applied cycle was thought to represent roughly the exposure to de-icing salt and dry intermittent periods in practice. At 30 weeks, small parts were sawn off for chloride profiling; the remaining parts were divided over three climates (two specimens per mix):

(i) a fog room (20 °C > 95% RH),
(ii) outdoors (unsheltered), and
(iii) a climate room at 20 °C and 80% RH.

Table 1
Cement types, w/c ratios and cement contents; $D_{max}$ 8 mm

| Mix code | Cement type | w/c | Cement content (kg/m$^3$) | Aggregate content (kg/m$^3$) | Water content (kg/m$^3$) | Admixture (% by mass of cement) |
|---|---|---|---|---|---|---|
| 1400 | CEM I 32.5 R | 0.40 | 338 | 1780 | 143 | 4.0 |
| 1450 | Portland cement | 0.45 | 318 | 1790 | 149 | 3.0 |
| 1550 | | 0.55 | 287 | 1827 | 163 | 3.0 |
| 2400 | CEM II/B-V 32.5 R | 0.40 | 333 | 1807 | 141 | 4.0 |
| 2450 | Portland fly ash cement | 0.45 | 314 | 1818 | 145 | 2.0 |
| 2550 | (27% fly ash) | 0.55 | 280 | 1830 | 158 | 2.0 |
| 3400 | CEM III/B LH HS 42.5 | 0.40 | 339 | 1836 | 141 | 2.5 |
| 3450 | blast furnace cement | 0.45 | 316 | 1831 | 146 | 2.0 |
| 3550 | (75% slag) | 0.55 | 286 | 1864 | 161 | 2.0 |
| 5400 | CEM V/A 42.5 compos- | 0.40 | 333 | 1827 | 137 | 2.0 |
| 5450 | ite cement | 0.45 | 322 | 1882 | 149 | 2.0 |
| 5550 | (25% fly ash, 25% slag) | 0.55 | 279 | 1839 | 157 | 2.0 |

Final measurements were taken 52 weeks after casting. Specimens exposed outdoors were taken inside and tested after about 4 h. This ensured that the concrete is at laboratory temperature, but the moisture content at the depth of the electrodes is about as it was outside.

Compressive strengths were determined at about 28 days of age. Chloride penetration was analysed by dissolving samples ground off in 2 mm increments in hot nitric acid of 3 molar strength and Volhard's titration. Optical microscopy was performed on samples taken near to where the chloride profiles were determined. They were impregnated with fluorescent resin and polished down to transparent "thin sections". The microstructure was described and the air void contents were estimated.

The resistance was measured between pairs of stainless steel electrodes using 120 Hz AC. The resistivity was obtained by multiplying the measured resistance [14] with a cell constant of 0.093 m for electrodes at 10 mm depth and 0.106 m for electrodes at 50 mm depth. Cell constants were obtained by calibrating with 100 mm cubes of identical composition with external steel plate electrodes. Electrodes at 10 mm depth provide information on the outer layers of the specimens, electrodes at 50 mm on the inner parts.

Potentials of the steel bars were measured using embedded Ti* reference electrodes. The corrosion rate was measured using the polarisation resistance technique (without ohmic drop compensation) with the three bars alternatively as working, reference and counter electrodes. Potentials more negative than approximately −300 mV are considered indicating active corrosion. For corrosion rates the following criteria are applied [14]: $< 1$ μm/a negligible; 1–5 μm/a low; 5–10 μm/a moderate; $> 10$ μm/a high.

## 3. Results

### 3.1. Concrete testing

Compressive strengths and air void contents are summarised in Table 2. Strengths are as expected. Air void contents of 2% are low, 2–5% moderate, 5–8% high, 8–15% very high. Microscopy showed that salt/drying exposure had not affected the microstructure negatively. Local inhomogeneities of the cement paste, relatively high air-void contents and a low degree of bonding between the matrix and aggregate particles were observed, caused by sub-optimum mixing and compaction.

### 3.2. Resistivity

Concrete resistivity was measured at ages 1, 2, 4, 5, 6, 8, 12, 16, 20, 24, 30 and 52 weeks. Fig. 2 shows the development for w/c 0.45 mixes. The resistivity increases during salt/dry cycles and then decreases when specimens are moved to the fog room (30→ 52 weeks). Values are given in Table 3 (for w/c 0.45 mixes), showing:

(a) after one week in the fog room, CEM III/B concrete shows the highest resistivity (125 Ωm), about two times higher than CEM V/A (60 m) and three times higher than CEM I and II/B-V (40 Ωm);

(b) after three weeks in air of 20 °C 80% RH, resistivity increases by a factor three to five; the increase is stronger at 10 mm depth than at 50 mm depth, mainly due to evaporation of pore water from the outer layers;

(c) after the first salt application (week 5), values at 10 mm first decrease due to wetting;

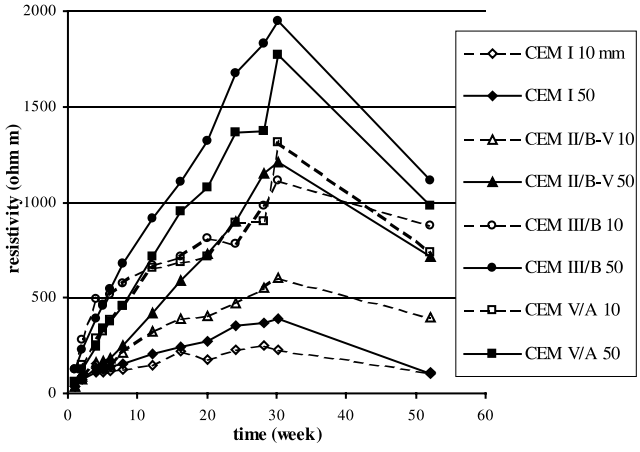


Fig. 2. Resistivity of 0.45 concrete (at 10 and 50 mm depth) during salt/drying cycles from week 4–30 and in the fog room at 52 weeks.

Table 2
Compressive strengths at about 28 days and air void contents (see text)

| | Compressive strength (N/mm²) | | | Air void content (% by volume) | | |
|---|---|---|---|---|---|---|
| Cement w/c | 0.40 | 0.45 | 0.55 | 0.40 | 0.45 | 0.55 |
| CEM I | 46 | 42 | 23 | 5–8 | 2–5 | 8–15 |
| CEM II/B-V | 53 | 41 | 37 | 5–8 | 5–8 | 5–8 |
| CEM III/B | 43 | 42 | 35 | 2–5 | 5–8 | 8–15 |
| CEM V/A | 61 | 46 | 36 | 2 | 2–5 | 2–5 |

Table 3
Resistivity of w/c 0.45 concretes (Ω m); −10 and −50 measured at 10 and 50 mm depth

| CEM type | Time since casting (week) | | | | | | | |
|---|---|---|---|---|---|---|---|---|
| | 1 | 4 | 5 | 16 | 30 | 52 | 52 | 52 |
| | Fog room | 20 °C 80%RH | Salt/dry cycles | | | Fog room | Outside | 20 °C 80%RH |
| I-10 | 38 | 136 | 112 | 220 | 232 | 112 | 217 | 285 |
| I-50 | 37 | 110 | 127 | 242 | 390 | 104 | 242 | 352 |
| II-B/V-10 | 35 | 164 | 137 | 388 | 603 | 401 | 971 | 910 |
| II-B/V-50 | 34 | 131 | 171 | 591 | 1209 | 713 | 1216 | 1442 |
| III/B-10 | 125 | 493 | 461 | 718 | 1114 | 881 | 1553 | 1439 |
| III/B-50 | 123 | 388 | 464 | 1111 | 1949 | 1118 | 1817 | 1997 |
| V/A-10 | 57 | 287 | 322 | 685 | 1317 | 741 | 1481 | 1539 |
| V/A-50 | 55 | 245 | 341 | 949 | 1772 | 978 | 1587 | 2128 |

(d) from about 8 weeks, CEM II/B-V resistivity increases markedly compared to CEM I, suggesting that hydration of fly ash starts to densify the matrix significantly;
(e) at about 30 weeks, all resistivities at 10 mm depth have increased by a factor 6–20 compared to values at one week; this is due to drying out and further hydration;
(f) at about 30 weeks, all resistivities at 50 mm depth have increased by a factor 10–30 compared to the value for one week, due to both drying out and further hydration; the drying out is stronger than at 10 mm depth;
(g) exposure for 22 weeks after the salt/dry cycles *in the fog room* increases the resistivity compared to values for one week by a factor 3 (CEM I), 12–21 (CEM II/B-V), 7–9 (CEM III/B) and 13–17 (CEM V/A); and,
(h) exposure for 22 weeks after salt/drying cycles *in 20 °C 80% RH* increases resistivity measured at 10 mm depth and decreases it at 50 mm depth for CEM I; increases resistivity measured at 10 mm depth and does not affect it at 50 mm in CEM III/B concrete; increases resistivity measured both at 10 and 50 mm depth in CEM II/B-V and CEM V/A concrete.

CEM III/B and CEM V/A have the highest resistivities at about one year of age. Apparently slag is able to produce very high resistivities, which starts at an early age for high slag percentages. Cement with a lower slag percentage and fly ash starts more slowly, but reaches very high values given the sufficient time and moisture. CEM II/B-V and CEM V/A mixes have shown the strongest increase since week 1 (a factor 10–15). Apparently the fly ash has increased the resistivity by densifying the pore structure. So far, 0.45 results were reported. The resistivities of CEM III/B and CEM V/A 0.40 mixes are very similar to values of their 0.45 counterparts. For CEM I and to a lesser extent for CEM II/B-V the resistivity of 0.40 is 20–50% higher than for 0.45. For 0.55 mixes, resistivities are lower than for 0.45, about a factor three when measured at 10 mm depth and a factor two at 50 mm.

### 3.3. Chloride penetration

Chloride profiles after 26 weekly salt/drying cycles are shown in Fig. 3 (each curve is the average of six specimens). All curves have a maximum at 3 or 5 mm depth; 1550 has a maximum at about 10 mm, with a very flat shape. The occurrence of a maximum may be due to the intermittent wetting/drying exposure. During wetting, chloride solution penetrates a layer of concrete; during the drying stage, the evaporation front moves inwards and takes some of the chloride with it. In addition, chloride may have been pushed inwards due to carbonation which liberates bound chloride. Carbonation depths found by microscopy of 2–3 mm support this.

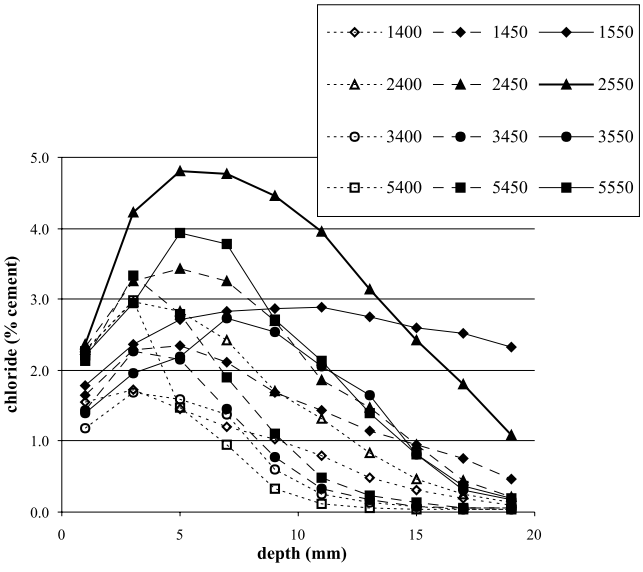


Fig. 3. Chloride profiles after 26 weekly cycles of 24 h 3% NaCl solution and 6 days drying in 20 °C 50% RH; each curve average of profiles from six specimens: codes '1' CEM I, '40' w/c 0.40, etc.

Table 4
Chloride content in the outer 20 mm in % by mass of cement and in accumulated amount (g) of chloride per $m^2$ of surface

| | Chloride in outer 20 mm (% by mass of cement) | | | Accumulated amount of chloride (g per $m^2$ of concrete surface) | | |
|---|---|---|---|---|---|---|
| Cement w/c | 0.40 | 0.45 | 0.55 | 0.40 | 0.45 | 0.55 |
| CEM I | 0.9 | 1.5 | 2.6 | 60 | 94 | 147[a] |
| CEM II/B-V | 1.5 | 2.0 | 3.3 | 101 | 125 | 185 |
| CEM III/B | 0.7 | 0.9 | 1.6 | 47 | 56 | 90 |
| CEM V/A | 0.8 | 1.2 | 2.0 | 55 | 79 | 114 |

[a] Total penetrated chloride probably 50% more due to penetration beyond 20 mm.

Table 4 displays the average chloride contents in the outer 20 mm and the accumulated amount of chloride per $m^2$ of concrete surface. The average contents vary over the mixes from 0.9% to 2%, with the lowest contents for 0.40 mixes made with CEM I, III/B and V/A (less than 1%), and the highest values for 0.55 CEM I and II/B-V mixes (up to 3%). The amounts of chloride are relatively low compared to long term coastal exposure data [15].

In particular, for specimens with a well-defined profile, the average content in 0–20 mm is too pessimistic with regard to corrosion of bars at 10 mm depth. Table 5 shows the average chloride contents from 8 to 12 mm depth, which is more representative. They will be discussed below. In addition, it shows the relative chloride content compared to CEM I 0.45 concrete. Compared to CEM I concrete with w/c 0.45, the chloride content is 40% lower for 0.40 and 100% higher for 0.55. Chloride contents at 8–12 mm depth are higher in CEM II/B-V and lower in CEM III/B and CEM V/A compared to CEM I concrete. In 0.55 concrete, the differences between cement types are smaller.

Diffusion profiles were calculated from the penetration profiles. The resulting chloride surface contents and diffusion coefficients are shown in Table 6. The calculated surface contents range from 2.3% to 5%. Those of CEM II/B-V and CEM V/A (4–5%) are higher than for CEM I and CEM III/B (2.3–3%), with small variations with w/c. The calculated apparent diffusion coefficients range from 1.4 to $10 \times 10^{-12}$ $m^2/s$. An exception is CEM I 0.55, with a much higher value, here reported as the average of two specimens as $140 \times 10^{-12}$ $m^2/s$. The profiles of the other four specimens were very flat, making it impossible to calculate a diffusion profile. The results show that CEM III/B and CEM V/A have the lowest diffusion coefficients for all w/c. Compared to CEM I, CEM II/B-V has a lower diffusion coefficient for 0.45 and 0.55, and a similar value for 0.40. For all mixes 0.40 has the lowest and 0.55 the highest diffusion coefficient. The difference between 0.40 and 0.45 for CEM III/B and CEM V/A is small.

It is realised that the experimental conditions do not represent true diffusion conditions, the latter occurring in fully saturated concrete. Despite this, the usual difference between cement types was noted [2]: CEM III/B apparent diffusion coefficients are significantly lower than CEM I values. It is interesting that CEM V/A is similar to CEM III/B and that CEM II/B-V takes an intermediate position. Differences between CEM II/B-V and CEM I are larger for higher w/c.

Table 5
Chloride content at 10 mm depth (slices 8–12 mm) in % by mass of cement and relative to CEM I 0.45 concrete

| | Average 8–12 mm (% by mass of cement) | | | Relative to CEM I 0.45 (–) | | |
|---|---|---|---|---|---|---|
| Cement w/c | 0.40 | 0.45 | 0.55 | 0.40 | 0.45 | 0.55 |
| CEM I | 0.9 | 1.6 | 2.9 | 0.6 | 1.0 | 1.9 |
| CEM II/B-V | 1.5 | 2.3 | 4.2 | 1.0 | 1.5 | 2.8 |
| CEM III/B | 0.4 | 0.6 | 2.3 | 0.3 | 0.4 | 1.5 |
| CEM V/A | 0.2 | 0.8 | 2.4 | 0.1 | 0.5 | 1.6 |

Table 6
Average surface content $C_s$ and apparent diffusion coefficient $D_{Cl}$ after 26 weekly salt/dry cycles

| | $C_s$ (%by mass of cement) | | | $D_{Cl}(10^{-12}$ $m^2/s)$ | | |
|---|---|---|---|---|---|---|
| Cement w/c | 0.40 | 0.45 | 0.55 | 0.40 | 0.45 | 0.55 |
| CEM I | 2.3 | 2.8 | 2.5 | 2.9 | 6.6 | 140[a] |
| CEM II/B-V | 3.9 | 4.1 | 4.9 | 2.9 | 3.7 | 9.2 |
| CEM III/B | 2.4 | 3.2 | 2.4 | 1.8 | 1.8 | 4.9 |
| CEM V/A | 4.5 | 4.8 | 3.8 | 1.4 | 1.8 | 3.9 |

$n = 6$ specimens, $n = 2$ specimens (see text).
[a] Except CEM I 0.55.

In additional experiments, diffusion profiles were calculated from the penetration profiles obtained from constant immersion of the 0.45 mixes in 3% NaCl solution. The results are discussed more fully in [16]. To summarise, there was good correspondence in terms of diffusion coefficients between immersion data for one year and the salt/drying data described above. This shows that although assuming diffusion transport for salt/dry exposure is theoretically incorrect, the resulting coefficients are realistic.

### 3.4. Steel potentials

Steel potentials in all specimens were quite negative after one week in the fog room (−400 to −700 mV versus Ti*, comparable to Ag/AgCl). This seems to suggest that the steel in all specimens is actively corroding, which contradicts normal experience. From two weeks of age on, potentials shifted to more positive values (about −100 mV), indicating that the steel had passivated.

During salt/drying exposure, potentials of steel bars at 10 mm depth shifted to more negative values. In Fig. 4 each data point is the average of 18 bars (three bars in six specimens). At about 30 weeks all bars in CEM I and CEM II-B-V specimens are corroding actively (potentials below −300 mV). In CEM III/B and CEM V/A, only a few bars are corroding. The number of corroding bars for the 0.45 mixes is shown in Table 7. Most bars at 10 mm cover depth corrode after salt/dry exposure for 26 weeks plus another 22 weeks (either in a fog room, outside or in 20 °C 80%RH). It is clear that the exposure has been very severe for bars at such low cover depth. At the end of the salt/dry exposure (week 30), it seems none of the bars at 30 mm depth was corroding. In week 52, 6 out of 18 bars were corroding in CEM II/B-V, CEM III/B and CEM V/A specimens (all in the fog room), and 9 bars out of 18 in CEM I specimens (fog room plus 20 °C 80% RH). This apparent transition from passive to active potentials is surprising. It could be related to movement of chloride and/or to low availability of oxygen in the fog room.

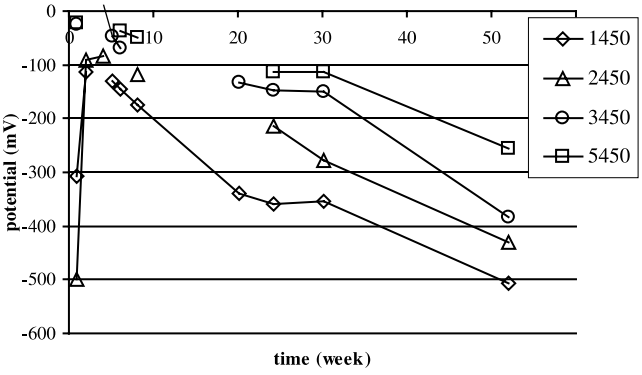


Fig. 4. Average potentials of 18 steel bars at 10 mm depth for 0.45 mixes during and after salt/dry cycles (from week 4 until 30); codes '1' CEM I, '45' w/c 0.45, etc.

The results of w/c 0.40 specimens are similar to those of 0.45. In 0.55 mixtures, almost all bars at 10 mm cover depth are corroding after 30 weeks, no bars at 30 mm are corroding. After 52 weeks, all bars at 10 mm corrode, all bars in CEM I 0.55 at 30 mm corrode and about half the bars at 30 mm in specimens made with the other cement types corrode.

The results are expressed as "probability of corrosion" in Table 8 and Fig. 5. This is the percentage of bars corroding out of 18 bars (total number of bars in specimens of each mix). The results show:

(a) from a certain point in time, the probability of corrosion exceeds 0%; for some mixes, it goes quickly up to 100%, other mixes show a more gradual increase over time;

(b) at about 30 weeks, the probability of corrosion is significant for CEM I and II/B-V (0.40), all cements (0.55) for bars at 10 mm depth and CEM I (0.55) for bars at 30 mm; and,

(c) at about 52 weeks, the probability of corrosion has increased for all cements and cover depths.

### 3.5. Corrosion rates

Corrosion rates at an age of one week are quite high (typically 20–50 μm/a), and for three more weeks still

Table 7
Number of bars corroding out of a total of 18 bars (potential more negative than −300 mV), 0.45 mixes

| Week | Depth | 10 mm | | | | 30 mm | | | |
|---|---|---|---|---|---|---|---|---|---|
| | CEM | I | II/B-V | III/B | V/A | I | II/B-V | III/B | V/A |
| 4 | | 0 | 0 | 0 | 0 | 0 | 0 | 0 | 0 |
| 5 | | 1 | 0 | 0 | | 0 | 0 | 0 | |
| 6 | | 2 | 0 | 0 | 0 | 0 | 0 | 0 | 0 |
| 8 | | 5 | 1 | | 0 | 0 | 0 | | 0 |
| 20 | | 14 | | 2 | | 0 | | 0 | |
| 24 | | 16 | 10 | 3 | 2 | 0 | 0 | 0 | 0 |
| 30 | | 16 | 15 | 4 | 2 | 0 | 0 | 0 | 0 |
| 52 | | 18 | 18 | 17 | 13 | 9 | 6 | 6 | 6 |

Table 8
Probability of corrosion in % at about 30 and 52 weeks for all mixes and cover depths

| w/c | 0.40 | | | | 0.45 | | | | 0.55 | | | |
|---|---|---|---|---|---|---|---|---|---|---|---|---|
| Cover (mm) | 10 | | 30 | | 10 | | 30 | | 10 | | 30 | |
| Time (week) | 30 | 52 | 30 | 52 | 30 | 52 | 30 | 52 | 30 | 52 | 30 | 52 |
| CEM I | 22 | 100 | 0 | 33 | 83 | 100 | 0 | 50 | 100 | 100 | 100 | 100 |
| CEM II/B-V | 61 | 89 | 0 | 33 | 33 | 100 | 0 | 33 | 100 | 100 | 0 | 56 |
| CEM III/B | 0 | 56 | 0 | 50 | 17 | 83 | 0 | 33 | 94 | 100 | 0 | 50 |
| CEM V/A | 0 | 22 | 0 | 33 | 0 | 33 | 0 | 33 | 78 | 100 | 0 | 39 |

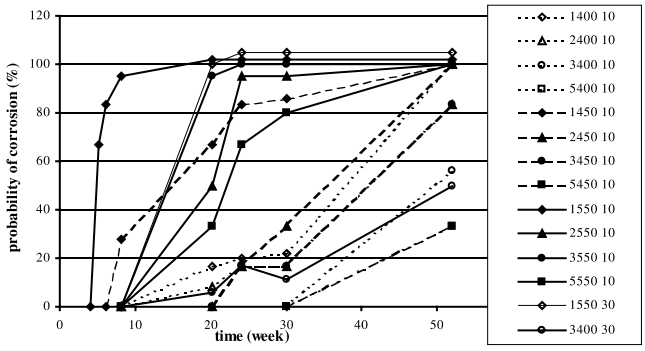


Fig. 5. Probability of corrosion during and after cyclic salt/dry exposure (week 4–30) of bars at 10 mm cover depth, some at 30 mm; codes '1' CEM I, '40' w/c 0.40, etc.

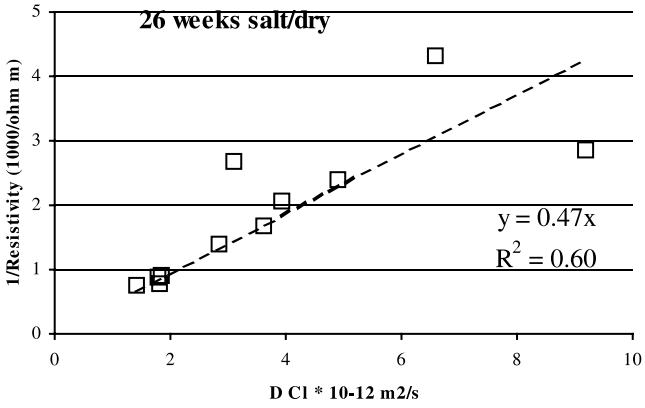


Fig. 6. Correlation between inverse resistivity and apparent diffusion coefficient.

relatively high but decreasing (typically 5–20 μm/a). These values are probably not representative for real corrosion of the steel, but may have to do with the process of passivation.

During the salt/drying cycles measurements have been taken only after 5, 6 and 8 weeks. There does not seem to be a systematic pattern in these data (most corrosion rates 5–10 μm/a). Subsequently they have been measured at 52 weeks. More details are given in [17]. To summarise, the highest corrosion rates occur in CEM I and CEM II/B-V concrete, for bars at 10 mm depth, and most strongly in 0.55 and 0.45 concrete, in the fog room and outside. In CEM III/B and CEM V-A concrete, only bars at 10 mm depth in 0.55 concrete show significant corrosion rates (>5 μm/a). Corrosion rates in CEM III/B and CEM V/A (bars at 10 and 30 mm depth) and of bars at 30 mm in CEM I and CEM II/B-V are insignificantly low (typically 1 to 3 μm/a). The influence of moisture is clear: corrosion rates in the fog room are higher than in 20 °C 80% RH or outside.

## 4. Discussion

During and after salt/dry cycling the resistivity was found to depend strongly on the cement type; increasing in the order CEM I < CEM II/B-V < CEMV/A < CEMIII/B. Also, the apparent chloride diffusion coefficients decrease in the order CEM I > CEM II/B-V > CEMV/A > CEMIII/B. According to [5] the inverse of resistivity is proportional to the chloride diffusion coefficient. This was confirmed for a wide range of concrete compositions during constant immersion [6]. For the present results Fig. 6 shows the inverse resistivity measured at 10 mm depth at about 30 weeks of age plotted versus $D_{Cl}$ as found after salt/dry exposure (except 1550). The correlation is reasonable and may be expressed as Resistivity × Diffusion coefficient = $A$, with $A$ constant. Compared to [6] and data from [18], the product A (here about $2000 \times 10^{-12}$, described in the plot by a line $y = 0.5x$) is a factor 4 higher. This is most probably caused by incomplete saturation of the concrete in the present experiments, both increasing the resistivity and/or increasing the rate of chloride ingress (involving some capillary absorption), which increases the value of the apparent diffusion coefficient.

Table 9 collects resistivities, steel potentials and corrosion rates of 0.45 mixes at about 52 weeks and chloride content at about 30 weeks. Throughout the data, higher resistivities were obtained in drier climates and these relate to lower corrosion rates. An inverse correlation between resistivity and corrosion rate was found in laboratory results and in coastal exposure [10,11]. Chloride contents in CEM I and II/B-V of 1.5–2% at 10 mm depth relate to higher corrosion rates. In CEM III/B

Table 9
Potential, corrosion rate and resistivity at about 52 weeks and chloride content at 8–12 mm depth at about 30 weeks

| 52 weeks | Fog room | | Outside | | 20 °C 80% RH | |
|---|---|---|---|---|---|---|
| Electrodes at (mm) | 10 | 30/50 | 10 | 30/50 | 10 | 30/50 |
| *Potential* (mV) | | | | | | |
| CEM I | −607 | −341 | −437 | **−111** | −478 | *−228* |
| CEM II/B-V | −531 | −362 | −388 | **−147** | −374 | **−92** |
| CEM III/B | −527 | −424 | −351 | **−134** | *−273* | **−91** |
| CEM V/A | −496 | −420 | *−258* | **−150** | −300 | **−47** |
| *Corrosion rate* (μm/a) | | | | | | |
| CEM I | 37 | 8.4 | 15 | 0.8 | 8.3 | 2.1 |
| CEM II/B-V | 18 | 3.3 | 5.7 | 0.8 | 5.3 | 1.0 |
| CEM III/B | 3.8 | 2.1 | 1.9 | 0.9 | 2.3 | 0.7 |
| CEM V/A | 3.1 | 1.9 | 1.5 | 1.9 | 1.6 | 0.7 |
| *Resistivity* (Ω m) | | | | | | |
| CEM I | 112 | 104 | 217 | 242 | 285 | 352 |
| CEM II/B-V | 401 | 713 | 971 | 1216 | 910 | 1442 |
| CEM III/B | 881 | 1118 | 1553 | 1817 | 1439 | 1997 |
| CEM V/A | 741 | 978 | 1481 | 1587 | 1539 | 2128 |
| Chloride content (% by mass of cement) at 8–12 mm depths at 30 weeks; average of six specimens per mix | | | | | | |
| CEM I | 1.56 | | | | | |
| CEM II/B-V | 2.28 | | | | | |
| CEM III/B | 0.56 | | | | | |
| CEM V/A | 0.80 | | | | | |

w/c 0.45; potential data: normal typeset indicates high corrosion risk, italic – intermediate, bold – low.

and V/A concrete they were 0.5–1%. Steel potentials suggest that these chloride contents have initiated corrosion of bars; corrosion rates are however relatively low. It appears that once corrosion has initiated due to chloride exceeding some threshold, the resistivity controls the corrosion rate, reflecting the moisture state. Steel potentials in the fog room correctly indicate active corrosion, but do not distinguish between (very) high corrosion rate (CEM I) and quite low values (CEM III/B and V/A). Similarly, potentials indicate active corrosion in 20 °C 80% RH (CEM I, II/B-V), but corrosion rates are quite low.

The probability of corrosion (from potential data) increases as a function of chloride content, which is illustrated in Fig. 7. Each symbol represents 18 bars (in six specimens). A straight line fits to the rising part of the curve through the symbols given by $y = 58x - 12$ ($R^2$ c. 0.90). At about 2% chloride by mass of cement, all bars probably corrode. Below 0.2% chloride, the probability is practically zero. At 0.3% chloride, the probability of corrosion is 5%.

The potential and corrosion rate data for bars at 30 mm depth suggest corrosion in the fog room in CEM I and possibly in CEM II/B-V. It is possible that depass-

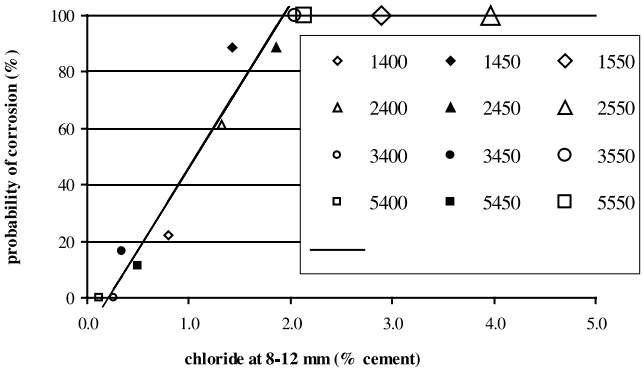


Fig. 7. Probability of corrosion as a function of chloride content for all mixes (from potential data at 30 weeks); codes '1' CEM I, '40' w/c 0.40, etc.

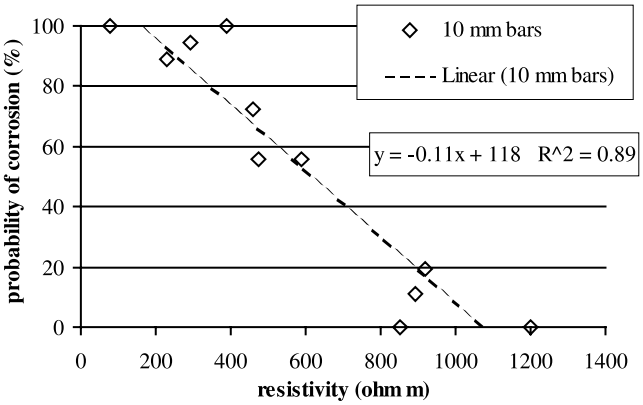


Fig. 8. Probability of corrosion at 24 weeks (after 20 weeks of salt/drying load) as a function of concrete resistivity; w/c 0.40, 0.45, 0.55.

ivating amounts of chloride have reached bars at 30 mm due to transport of chloride during the 22 weeks in the fog room. On the other hand, it could be an artefact related to the low availability of oxygen in concrete in the fog room.

In Fig. 8 the correlation between resistivity and probability of corrosion is shown, considering data at about 24 weeks. It shows that a higher resistivity correlates well with a low probability of corrosion.

## 5. Conclusions

The experiments have shown that under simulated de-icing salt load, concretes made with CEM III/B (high percentage of blast furnace slag) and CEM V/A (intermediate levels of slag and fly ash) show less chloride penetration, lower probabilities of corrosion and higher electrical resistivities than concrete made with CEM I (ordinary Portland cement). CEM II/B-V (with an intermediate percentage of fly ash) concrete takes an intermediate position. With CEM II/B-V there is a strong influence of time: during the first eight weeks, its resistivity is very similar to that of CEM I. From about eight weeks of age, the resistivity of CEM II/B-V concrete becomes increasingly higher than that of CEM I concrete and in the long term may resemble a (high percentage) blast furnace slag cement. The influence of w/c ratio is limited for w/c 0.40 and 0.45; it is larger for w/c 0.55. The 0.55 mixes show a significantly lower resistivity and greater chloride penetration than their 0.45 counterparts. The 0.55 concrete, however, was poorly compacted.

For a wide range of concrete compositions in terms of cement type and w/c ratio, it appears that the electrical resistivity of a particular concrete reflects its properties with regard to chloride penetration under simulated de-icing salt load. The high chloride penetration resistance of blended cements in marine environment is also found under simulated de-icing salt conditions.

## Acknowledgements

This study was supported by ENCI N.V. and the Netherlands Ministry of Economic Affairs. The involvement of Mrs. Irene Dekker and Mrs. Sabine Bongen of ENCI N.V. is gratefully acknowledged. Mrs. Paola Russo of Universita La Sapienza, Rome is thanked for starting up the experiments within the framework of COST 521 "Corrosion of steel in reinforced concrete structures".

## References

[1] Polder RB, Larbi JA. Investigation of concrete exposed to north sea water submersion for 16 years. HERON 1995;40(1):31–56.
[2] Polder RB. The influence of blast furnace slag, fly ash and silica fume on corrosion of reinforced concrete in marine environment. HERON 1996;41(4):287–300.
[3] Gjørv OE, Vennesland Ø, El-Busaidy AHS. Electrical resistivity of concrete in the oceans. In: Ninth Annual Offshore Technology Conference, Houston, Paper 2803, 1977.
[4] Tuutti K. Corrosion of steel in concrete. CBI Stockholm; 1982. 468 pp.
[5] Andrade C, Sanjuan MA, Alonso MC. Measurement of chloride diffusion coefficient from migration tests. In: Paper 319, NACE Corrosion'93, 1993.
[6] Polder RB. Chloride diffusion and resistivity testing of five concrete mixes for marine environment. In: Nilsson L-O, Ollivier P, editors. Proceedings of the RILEM International Workshop on Chloride Penetration into Concrete, St-Remy-les-Chevreuses, RILEM. 1997.
[7] Schiessl P, editor. Corrosion of steel in concrete RILEM Technical Committee 60-CSC. London: Chapman & Hall; 1988.
[8] Bazant Z. Physical model for steel corrosion in concrete sea structures part theory part application. J Struct Div Am Soc Civil Eng 1979;105(ST6):1137–66.
[9] Alonso C, Andrade C, Gonzalez J. Relation between resistivity and corrosion rate of reinforcements in carbonated mortar made with several cement types. Cem Concr Res 1988;18:687–98.
[10] Glass GK, Page CL, Short NR. Factors affecting the corrosion rate of steel in carbonated mortars. Corros Sci 1991;32:1283–94.
[11] Polder RB, Bamforth PB, Basheer M, Chapman-Andrews J, Cigna R, Jafar MI, Mazzoni A, Nolan E, Wojtas H. Reinforcement corrosion and concrete resistivity-state of the art laboratory and field results. In: Swamy RN, editor. Proceedings of the International Conference on Corrosion and Corrosion Protection of Steel in Concrete. Sheffield Academic Press; 1994. p. 571–80.
[12] Fiore S, Polder RB, Cigna R. Evaluation of the concrete corrosivity by means of resistivity measurements. In: Page CL, Bamforth PB, Figg JW, editors. Proceedings of the Fourth International Symposium on Corrosion of Reinforcement in Concrete Construction, Society of Chemical Industry, Cambridge, UK, 1–4 July, 1996. p. 273–82.
[13] Bertolini L, Polder RB. Concrete resistivity and reinforcement corrosion rate as a function of temperature and humidity of the environment. TNO report 97-BT-R0574, 1997, 85 pp.
[14] COST 509. Corrosion and protection of metals in contact with concrete, Final report. In: Cox, RN, Cigna R, Vennesland O, Valente T, editors. European Commission, Directorate General Science, Research and Development, Brussels, EUR 17608 EN, ISBN 92-828-0252-3, 1997, 148 pp.
[15] Vennesland Ø, Havdahl J. Field tests of concrete with microsilica. In: Eurocorr'99, Aachen, August 30–September 3, 1999.
[16] Polder RB. Simulated de-icing salt exposure of blended cement concrete Chloride penetration. In: RILEM TMC 178 Workshop, Paris, September 11–12, 2000.
[17] Polder RB, Peelen W. Simulated de-icing salt exposure of blended cement concrete corrosion aspects. In: Eurocorr 2000, London, September 10–14, 2000.
[18] Bamforth PB, Chapman-Andrews J. Long term performance of RC elements under UK coastal conditions. In: Swamy RN, editor. Proceedings of the International Conference on Corrosion and Corrosion Protection of Steel in Concrete. Sheffield Academic Press; 1994. p. 139–56.